Journal of the Physical Society of Japan
Vol. 53, No. 8, August, 1984, pp. 2491–2500

Total Cross-Sections for Positrons and Electrons Colliding with N_2, CO and CO_2 Molecules

Osamu SUEOKA and Shigeki MORI

Institute of Physics, College of Arts and Sciences, University of Tokyo, 3-8-1 Komaba, Meguro-ku, Tokyo 153

(Received January 30, 1984)

Total cross-sections for 1.0–400 eV positrons and 1.2–403 eV electrons colliding with N_2, CO and CO_2 molecules have been measured using a retarding potential-TOF technique. Results of positron-collisions for e^+-CO have shown clearly the Ramsauer-Townsend minimum. But the minimum was not shown clearly for e^+-N_2 and e^+-CO_2. These data were compared recent experimental data. Total cross-sections of electron-collisions were measured by the same technique for the comparison with those of positron-collisions, and they were compared with prior experimental data.

§1. Introduction

Many collision-experiments for low and intermediate-energy positrons colliding with gases have been reported since the moderator, by which a small fraction of fast positrons ejected from the pair creation[1] or the radio-isotope[2] was converted to low-energy positrons, was developed. A number of total cross-sections for low-energy positrons colliding with atoms and molecules have been measured by several groups.[3-6] The positron atom interaction in low-energy regions has been understood well by many experimental and theoretical studies in the case of simple gases. The agreement among experimental data, however, is not well and the number of the measurement except for noble gases is not so many. These discrepancies may be caused by the reason that measurements were carried out using a variety of techniques under the condition of low-intensity beams.

The interaction in positron-gas collision is founded on the polarization interaction between a positron and the induced dipolemoment, and on the static Coulomb interaction of a positron with the screened nucleus. The former interaction is attractive and the latter is repulsive. Because of these interactions the theoretical calculation must be performed accurately, though the exchange interaction does not exist. At the low-energy region for positron-gas collisions, total cross-sections Q_t^+ are low because the static Coulomb and the polarization interactions cancel each other. On the other hand, for electron-gas collisions total cross-sections Q_t^- are high because two kinds of the interaction add. These results are clearly shown in the measurement at the low-energy region below the threshold of positronium formation.

In this paper, measurements of the total cross-sections for 1.0–400 eV positrons colliding with N_2, CO and CO_2 molecules were performed using a retarding-potential time-of-flight method (RP-TOF).[7] We have reported a preliminary work for e^+-N_2 and e^+-CO by this technique.[7] But data presented here were independently obtained again. Data of the total cross-section were mainly compared with those of the Wayne State University group[8,9] and those of the University College group.[10] Measurements of total cross-sections for electrons colliding with the same gases have been performed also for the comparison with the data of positron-collisions by means of the same apparatus using a β^--decay electron source, Cs^{137}, instead of Na^{22} positron source. Values of the total cross-section in electron-gas collisions were obtained with enough accuracy, except the measurement of the shape resonance with the sharp energy-structure. The total cross-sections in positron-gas collisions were compared with those in electron-gas collisions to check of the similarity and the discrepancy on the same experimental conditions.

§2. Experimental Procedures and Arrangements

2.1 *Apparatus*

A straight-beam-type apparatus with a flight path of 692 mm length was constructed for the measurement of total cross-sections and for that of inelastic collisions for positron-gas collisions. The schematic diagram is shown in Fig. 1. The length of the collision cell, 79.7 mm, is rather short on purpose to be used in inelastic collision measurements. This value is the effective length, 18% larger than the geometrical length, and will be discussed later. Collision gases are exhausted by two-steps differential pumping. Solenoid coils for guiding of projectile particles in the flight path and water-cooling pipes for the solenoid coils are contained in the vacuum vessel for convenience. The magnetic field by the solenoid is 9 G in the collision cell, and that in the main flight path is 45 G. The power for the magnetic field is 6.5 VA. The increase of temperature by current in the solenoid coil is less than 10°C in the continuous use. The large pumping-speed system was used to overcome many obstacles in the vacuum chamber and the short collision-cell. The vacuum vessel was kept in 4×10^{-5} Pa in the vacuum run, and was kept better than 6×10^{-4} Pa in the gas run at the detecter chamber. The pressure in the collision cell was measured by a "Convectron vacuum gauge" manufactured by Granville-Phillips Co. The output signal of the gauge to a recorder is stable and sensitive enough for the use in order of $1-10^{-1}$ Pa, even the gauge is a kind of Pirani gauge. The output signal was connected to a

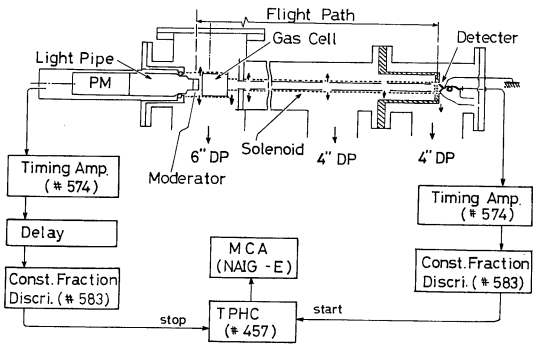

Fig. 1. Schematic diagram of the experimental arrangement and timing electronics.

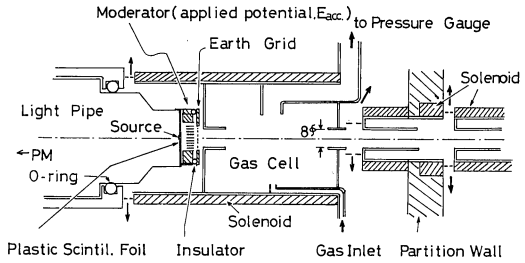

Fig. 2. Detail of the collision cell and the source part of projectile particles.

regulator for the pressure of collision gases. The vacuum gauge was carefully calibrated by a mercury-MacLeod gauge at the start and the end of each measurement. The pressure in the collisions cell was measured at the center of the cell only. The diameters of two apertures of the cell are 8 mm. Details of the cell was shown in Fig. 2.

The magnetic field due to solenoids brings the ambiguity in the total cross-section in low-energy regions. The intensity of low-energy positrons in the low solenoid-field decreases in the flight path by the terrestrial magnetism. At the vicinity of the collision cell, the terrestrial magnetism was reduced to less than 10% of the natural value by Helmholtz coils.

2.2 *Slow-positron and electron source*

A radioactive sodium-22 with an activity of about 60 μCi was used as a positron source. A fast positron detector, by which one of the timing marks is provided to the TOF circuit, consists of a plastic scintillator foil of 120 μm thick, a light pipe and a photomultiplier. The surface of the scintillator foil is evaporated by aluminum for high reflection of emitted light. The scintillator probe is inserted in vacuum. Fast positrons passed through the scintillator foil hit the moderator on which a small fraction of fast positrons is converted to low-energy positrons.

The moderator of heated tungsten-ribbons developed by Dale *et al.*[11] was used. Though the efficiency of slow positrons is not unstable, a set of W-ribbons moderator was baked out sometimes by direct current of 250 Amp. for baking of DP-oil contamination. At the initial stage of this experiment, a copper fine-mesh coated with MgO smoke was used as a moderator, but the conversion rate to low-energy

positrons was about 1/20 of that by the W-ribbons moderator.

Positrons ejected from the moderator are accelerated by E_{acc} potential as shown in Fig. 2. The half width of the energy distribution of slow positrons ejected from the moderator is 1.5–2.0 eV, depends on the value of E_{acc}, and on the condition of surfaces and geometry of W-ribbons. In the case that the moderator was used for long time, the energy width in the low energy side of the spectrum increased with increasing DP-oil contamination. The average energy of positrons E_p is about 0.7 eV + E_{acc}.

A radioactive cesium-137 with activity of 40 μCi was used as a electron source. It is supposed that low-energy electrons are obtained *via* many-fold scattering on W-ribbons moderator with increasing secondary electrons. The intensity of low-energy electrons is about 500 counts/sec, two-order stronger than that of slow-positrons. The energy spectrum of the slow-electron beam has wide energy-breadth with long slope in the high-energy side. The spectra of two kinds of the projectile particle will be shown in the paper of total cross-sections for $e^{\pm}$-CH_4, C_2H_4 and C_2H_6 (to be submitted).

2.3 *Detector and electronics*

For the detection of projectile particles, a ceratron manufactured by Murata MFG Co. Ltd., a sort of continuous dynode electron multiplier (CEM) was used. The detector must be used under the best detection-efficiency, because of low intensity of positron beams. The efficiency curve for a ceratron, the counting rate vs the impact energy to the cone of CEM, shows a fairly sharp peak than that for CEM manufactured by Galileo Electro-Optics Corp.[12] But the ceratron has several merits; low noise, able to be used even in worse vacuum (in order of 10^{-3} Pa), to be recovered easily by baking when it is dameged by discharge, and low cost.

The electronic circuit used in this experiment is a standard TOF system for fast pulse as shown in Fig. 1. The FWHM of the prompt curve for annihilation γ rays in this system is 4 n sec in the case of using short delay-cable. The typical CEM counting rate 15 counts/sec in vacuum run, which is 3×10^{-4} times lower than the scintillator counting rate. To avoid loss of the signal events by system busy time, the CEM pulses are used to start the TOF timing sequence, and the scintillator pulses delayed appropriately are used to stop. So, the time spectrum recorded in MCA is inverted.

2.3 *RP-TOF method*[7]

The time spectrum on the measurement in the intermediate-energy region involves inelastic contributions and the forward scattered intensity due to elastically scattered positrons with reduced axial velocities resulting from angular deflection. Because the energy resolution of TOF is bad at higher-energy regions, careful analysis is needed in order to obtained unscattered intensity from raw data.[13] For the elimination of these contributions caused by scattered positrons, one of the authors (O.S.) has developed the retarding potential-TOF (RP-TOF) method. This method was only accomplished by insert of a retarding grid in front of the detector. Even in the energy region where the inelastic scattering does not exist, the RP-TOF is useful to decrease the forward scattered contributions with reduced axial velocities. The contribution of elastic scattering with very small scattering angle, of course, is not eliminated from raw data for any method. It has been demonstrated that the RP-TOF method is useful in the measurement of total cross-sections in e^+-N_2 and e^+-CO collisions. In this experiment, $E_0 = 1.5$ eV for positron experiments and $E_0 = 0$ eV for electron experiments. Where E_0 is the difference between the accelerate potential E_{acc} and the retarding potential.

2.5 *Data analysis*

True time spectra in TOF data were obtained by the correction of the accidental coincidence using the formula by Coleman *et al.*[14] The number of the start pulse that is essential in the correction was determined by calculation of the time region in which real signal events are not expected to occur because the direct measurement of the number is not easy in our apparatus, while Charlton *et al.*[10] obtained the number using electronics directly. The correction of accidental coincidence was

carried out in enough accuracy in every energy range.

The total cross-section Q_t is computed from two numbers: $N_v=\sum_i n_{vi}$, $N_g=\sum_i n_{gi}$, according to

$$Q_t=-\frac{1}{\rho L}\ln(N_g/N_v). \quad (1)$$

Where ρ is the number density of gas in the collision cell and L is the effective length of the collision-cell, 79.7 mm. n_{vi} is the counts in i-th channel in the vacuum run, n_{gi} is that in the gas run. The summation is taken in full range of the unscattered peak in the case of impact energies larger than 12 eV for positron collisions and larger than 50 eV for electron collisions. For the lower impact energy ranges, the summation to the relevant energy is taken in part of the unscattered peak. In the higher energy ranges, the energy resolution is decided mainly by the energy breadth of the original spectrum of projectile particles emitted from the moderator, about 2 eV in the present case. In the energy ranges lower than 10 eV the resolution is about 0.5 eV for positrons, and about 0.3 eV for electron beams.

The total cross-section determined by eq. (1) must be independent on the collision-gas pressure. The check of the independence on gas pressure is also useful to know the the reliability of the experimental system. Especially, the check of the balance between the pressure in the collision cell and the exhaust pumping system is important, because our apparatus has the short collision cell with two

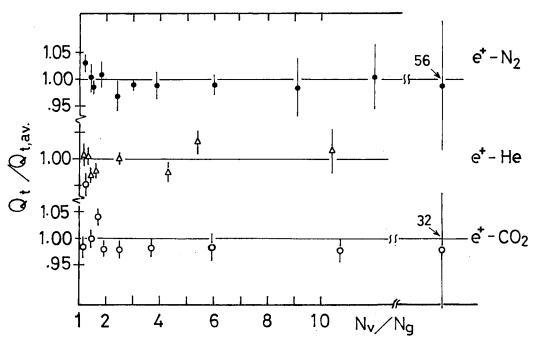

Fig. 3. Normalized total cross-sections plotted against beam intensity attenuation (N_v/N_g). Measurements in practical cases were performed in the range 2 to 4. Error bars show errors due to the intensity of positron beams ΔI only.

large exit apertures. This check means the independence of the effective length L on the pressure. As plotted in Fig. 3 it is permitted to use the constant value for L. The check was performed by other group to their apparatus.[8,10,15] Moreover, it may be resulted from the above facts that L is also independent on the kind of specimen-gas.

The value of the effective length L was decided by the normalization of the total cross-section for e^+-N_2 with those of Hoffman *et al.*[8] at 100–400 eV where the effect of the forward scattering was small.

2.6 *Evaluation of error*

In the present measurement large errors are come from the low intensity of positron beam. Namely, the forward scattering causes the main systematic error. Assuming uniform density of slow positrons at the moderator, the averaged perpendicular radius $\bar{r}_\perp$ of the positron spiral-motion in the magnetic field is deduced to $\bar{r}_\perp=1/3r_m$, where r_m is the radius of the exit aperture, i.e. 4 mm for the present apparatus. Using the value of the magnetic field $B=9$ G, the maximum angles of the forward elastic scattering θ_{mag} are 14.6, 6.5 and 2.0 degree for 2, 10 and 100 eV, respectively.

Though the RP-TOF method makes use of decrease of the forward scattering by retarding potential even in the energy range lower than the threshold of the inelastic scattering in principle, the decrease is not so effective because the retarding potential is selected to $E_0=$ 1.5 eV in this experiment. Although in the measurement of electron collisions, $E_0=0$ eV, the reduction of the forward scattering using the RP-TOF is not so decisive because the energy breadth of the electron source is very wide. The effect of the inelastic scattering, of course, is eliminated completely by the RP-TOF. We checked the quantity of the forward scattered intensity due to elastically scattered positrons with reduced axial velocities resulting from angular deflection in the time spectrum of MCA by the method of Coleman *et al.*[13] Because the quantity looks like very small though the reason is not known, we may deduce the decrease in the value of total cross-sections due to the forward scattering is not so large. The systematic error based to the for-

ward scattering is not included in the value of errors in the figures.

The error was evaluated by linear addition of the following three quantities.

1. Error of beam intensity ΔI. The statistical error in the intensity measurement was typically 1.3–2.0% for positron beams and 0.2–0.5% for electron beams.
2. Error of the density of collision gases $\Delta\rho$. The accuracy of the pressure in the collision cell bases mainly on a Convectron pressure-gauge and on its calibration. The accuracy of the calibration which was estimated by the reproducibility is not good in low pressure regions. The error due to a Convectron gauge and due to the calibration by a mercury-MacLeod gauge were estimated to 2.5–5%. Variation of room temperature was within 0.5°C during a measurement and that of the pressure of the collision gas was within 0.5%. The error $\Delta\rho$ was obtained by statistical summation.
3. Error in the determination of the length of the collision cell ΔL. The effective length L was determined by the normalization of the values of the total cross-sections to those for e^+-N_2 of Hoffman *et al.*[8] The direct error of the normalization is about 1%. If the normalization is performed for e^--N_2 in the energy range from 100 to 400 eV to data of Blaauw *et al.*,[16] the value of L decreases 10%. Taking into consideration of the reproducibility of data in an independent run, the value of $\pm 4\%$ was estimated as the maximum error. Namely, the value of ΔL involves uncertainty in the present experimental system. One of the cause of this error comes from the instability of beam intensities. Although sources of e^+ and e^- are the isotope, the beam intensity was not constant perfectly in some case. We suppose on the instability that the surface state of the moderator effects delicately to the pulse height.

§3. Results and Discussion

3.1 e^+-N_2 and e^--N_2

The total cross-sections for positrons with energies in the range 1 to 20 eV colliding with N_2 molecules are given in Fig. 4 along with recent experimental results[8,10] and theoretical results.[17–19] The minimum of the total cross-section in low-energy regions which corresponds to the Ramsauer-Townsend minimum is not shown clearly, like as data of Charlton *et al.*[10] On the other hand, the data of Hoffman *et al.*[8] which were measured with very high energy resolution, have been shown clearly the minimum: $Q^+_{\min}=3.0\times10^{-16}$ cm^2 at 3.0 eV. Recently, Darewych[19] has presented

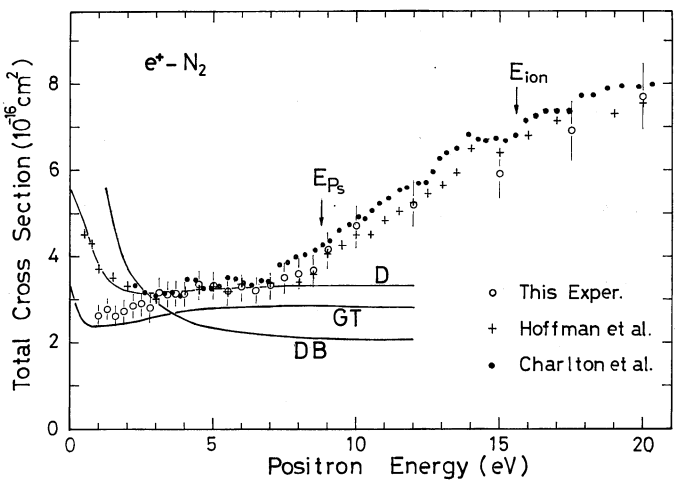

Fig. 4. Total cross-sections for positrons colliding with nitrogen molecules at low-energies. The present results are shown with the experimental data of Hoffman *et al.* (ref. 8) and Charlton *et al.* (ref. 10). Three theoretical curves DB, GT and D are elastic cross-sections calculated by Darewych and Baille (ref. 17), Gillespie and Thompson (ref. 18), and Darewych (ref. 19), respectively. Error bars show uncertainties of the present results except the error due to forward elastic scattering. The thresholds for positronium formation and ionization are indicated by arrows.

the integrated elastic total cross-section based on a single-center formalism. The theoretical curve coincides very well with the experimental values. Especially, the curve agrees with data of Hoffman *et al.* in the low-energy region. The experimental and theoretical minimum are very shallow just like as that for e^+-rare gases. Our data do not contradict these results. Except values in the energy range lower than 3 eV, data are in good agreement with those of refs. 8 and 10.

It is rather reasonable that a distinct hump is not found at the threshold of positronium formation ($E_{Ps}=8.8$ eV), because the positronium contribution to the total cross-section is deduced to give a gradual increase with increasing the positron energy.[20,21]

Data for e^+-N_2 in intermediate-energy ranges were plotted in Fig. 5 with prior experimental results.[7,8,22,23] Although data obtained are normalized to those of Hoffman *et al.*[8] at the energy between 100 and 400 eV, those show in fairly good agreement with data of Hoffman *et al.* as a whole. The data of Coleman *et al.*[24] which are one of the pioneer work in this study show fairly lower values than the data shown in Figs. 4 and 5. The tendency in the data of Coleman *et al.* is presented on data for e^+-CO and e^+-CO_2 also. Data in ref. 7 involve the mistake in estimation of the effective length of the collision cell L. Data of ref. 7 was corrected using new value of L. The effect on the total cross-section due to the magnitude of magnetic field for guide of projectile particles will be discussed elsewhere.

The total cross-sections for electrons in energy ranges higher than 5 eV colliding with N_2 molecules are presented in Fig. 6 along with those of Hoffman *et al.*,[8] those of Blaauw *et al.*[16] and those of Dalba *et al.*[25] Data obtained agree roughly with other data, but the peak at 20 eV is fairly higher than those. The total cross-sections for energies lower than 4.5 eV are shown in Fig. 7(a) with those of Hoffman *et al.*,[8] of Kenerly,[26] and theoretical data of Chandra and Temkin.[27] The reason why the peak at 2.4 eV due to the shape resonance is very low in comparison with all other data, bases on bad energy resolution in our measurement. The average perpendicular energy to the flight-path direction, $E_\perp$, is 0.75 eV in our electron source. The energy peak in the time spectrum of MCA is presented at the energy position of 0.75 eV lower than the energy of the shape resonance. The phenomena were observed also in the spectra for e^--CO, e^--CO_2 and e^--C_2H_4 (to be submitted). Except the fine structures of the shape resonance, total cross-section results were obtained with fairly good accuracy.

As indicated on the data in Figs. 5 and 6,

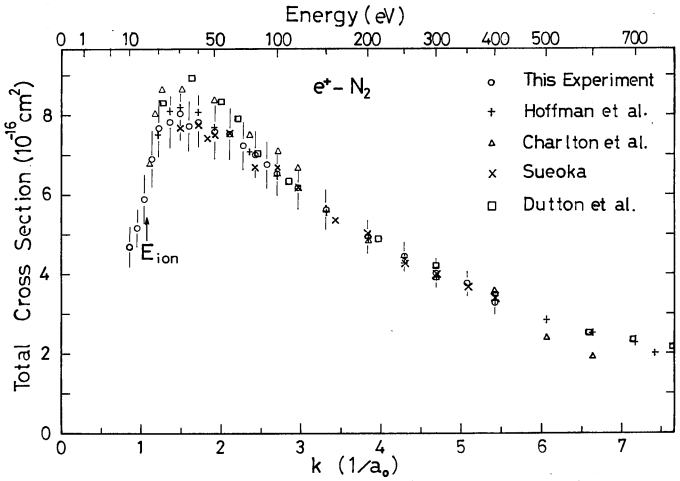

Fig. 5. Total positron—nitrogen molecule collision cross-section results extending to intermediate energies. The present results are shown with the experimental data of Hoffman *et al.* (ref. 8), Charlton *et al.* (ref. 22), Sueoka (ref. 7) and Dutton *et al.* (ref. 23). The threshold for ionization is indicated by an arrow.

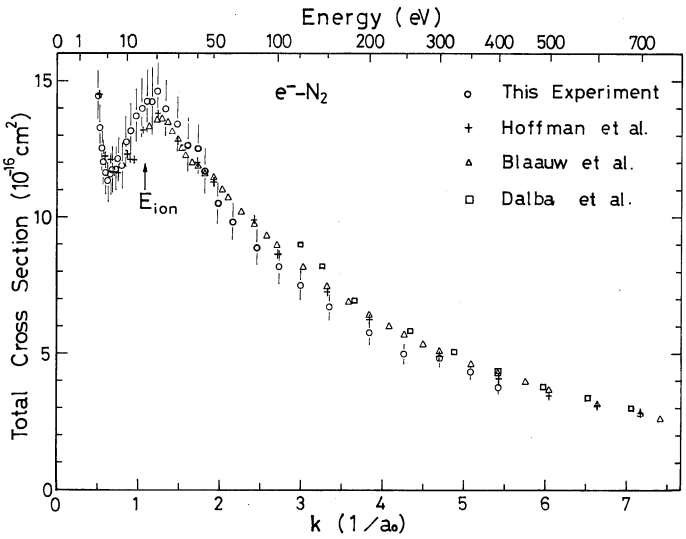

Fig. 6. Total electron—nitrogen molecule collision cross-section results extending to intermediate energies. The present results are shown with the experimental data of Hoffman *et al.* (ref. 8), Blaauw *et al.* (ref. 16) and Dalba *et al.* (ref. 25).

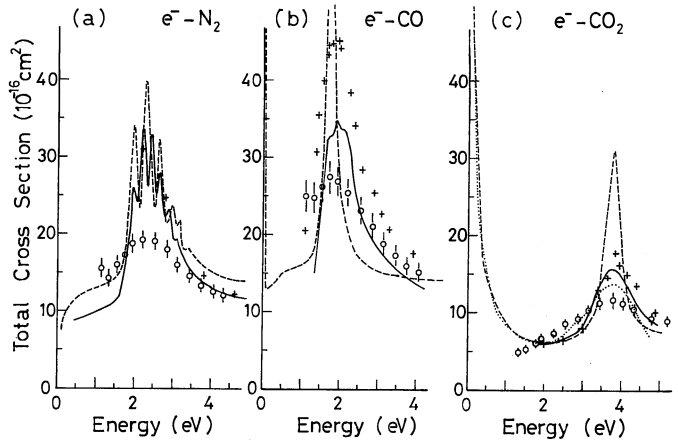

Fig. 7. Total cross-section results for e^--N_2, e^--CO and e^--CO_2 at low energies in (a), (b) and (c), respectively. The experimental data of Hoffman *et al.* (ref. 8), +; Kennerly (ref. 26), — curve; and the theoretical data of Chandra and Temkin (ref. 27), – – – curve are shown in (a) with the present data, ○. The experimental data of this work, ○; Kwan *et al.* (ref. 9), +; Szmytkowski and Zubek (ref. 29), — curve; and the theoretical data of Chandra (ref. 30), – – – curve are shown in (b). The experimental data of this work, ○; Hoffman *et al.* (ref. 8), +; Ferch *et al.* (ref. 31), ... curve; Szmytkowski and Zubek (ref. 2), — curve; and the theoretical data of Morrison *et al.* (ref. 32), – – – curve are shown also in (c).

the values of total cross-sections for e^--N_2 are fairly larger than those for e^+-N_2 even at intermediate energies. The same tendency is shown in the data for $e^{\pm}$-CO and $e^{\pm}$-CO_2. While for He the values of positron collisions and electron collisions are in good agreement in the energy range above 150 eV.[28] The comparison of the total cross-section for positron-gas collisions with that for electron collisions will be discussed in detail elsewhere.

3.2 e^+-CO and e^--CO

Total cross-sections for low and intermediate-energy positrons colliding with CO molecules are given in Figs. 8 and 9 with preliminary data[7] and those of Kwan *et al.*[9] The

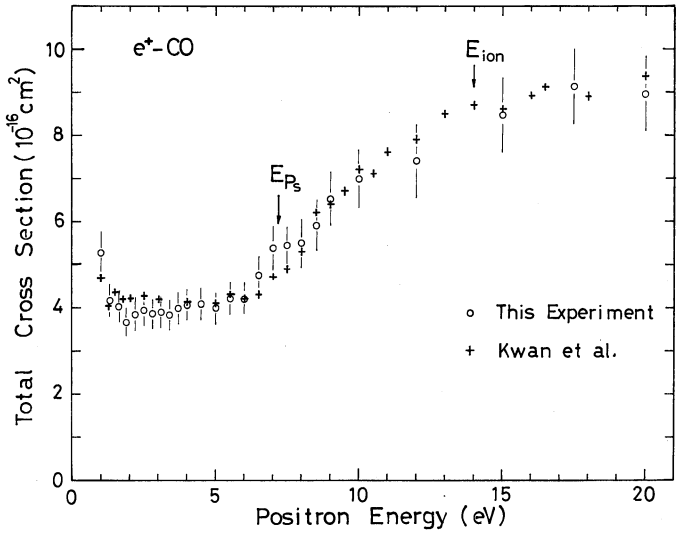

Fig. 8. Total e^+-CO scattering cross-section results at low energies. The present results are shown with the experimental data of Kwan *et al.* (ref. 9). Arrows show the thresholds for positronium formation and ionization.

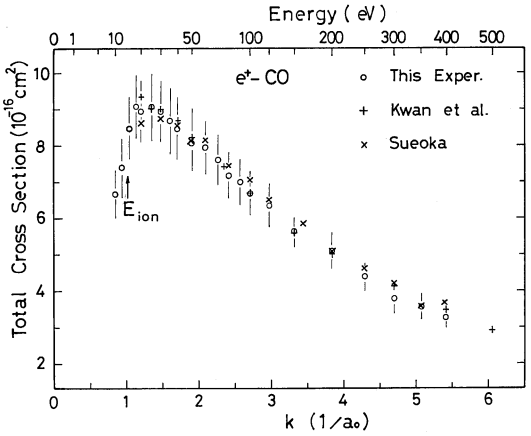

Fig. 9. Total positron—carbon-monooxide molecule collision cross-section results extending to intermediate energies. The present data are shown with the experimental data of Kwan *et al.* (ref. 9). The threshold for ionization is indicated by an arrow.

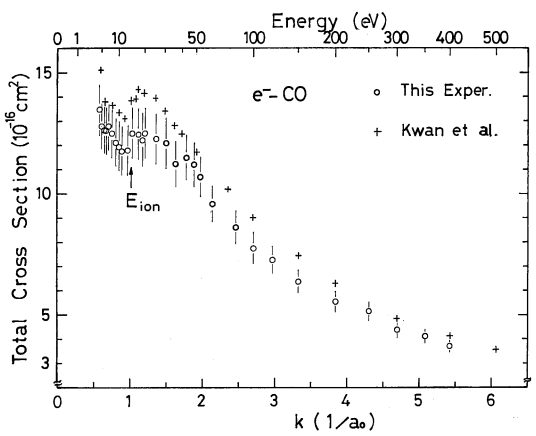

Fig. 10. Total electron—carbon-monooxide molecule collision cross-section results extending to intermediate energies. The present results are shown with the experimental data of Kwan *et al.* (ref. 9). The threshold of ionization is indicated by an arrow.

Ramsauer-Townsend minimum is shown as a very shallow minimum at 2–4 eV. The minimum value Q^+_{min} is 3.9×10^{-16} cm^2, and that by Kwan *et al.* is 4.1×10^{-16} cm^2 at 3–5 eV. Results obtained are good agreement with those of Kwan *et al.* A small hump at 7 eV is perhaps fluctuation of data.

Total cross-sections for electrons with energies in the range higher than 5 eV are shown in Fig. 10 with those of Kwan *et al.*[9] Data for lower energy ranges are shown in Fig. 7(b) with those of Kwan *et al.*, of Szmytkowski *et al.*[29] and theoretical values of Chandra.[30] By the same reason mentioned in the paragraph of e^--N_2, results obtained do not show quantitatively the shape resonance. The reason why our results in the high energy region are fairly small in comparison with those of Kwan *et al.* can not be explained.

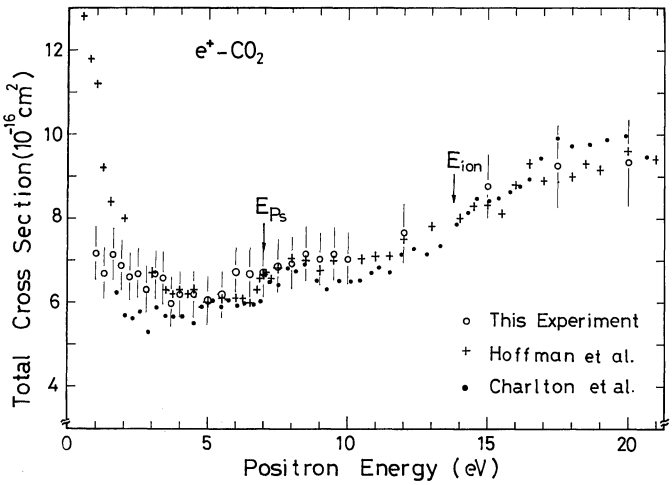

Fig. 11. Total positron—carbon-dioxide molecule collision cross-section results at low energies. The present results are shown with the experimental data of Hoffman *et al.* (ref. 8) and those of Charlton *et al.* (ref. 10). The thresholds for positronium formation and ionization are shown by arrows.

3.3 e^+-CO_2 and e^--CO_2

Values of the total cross-section for positrons with energies in the range from 1 to 20 eV are given in Fig. 11 with those of Hoffman *et al.*[8] and those of Charlton *et al.*[10] Data for positrons with energies in the range from 20 to 400 eV are given in Fig. 12 with those of Kwan *et al.*[9] and those of Charlton *et al.*[22] The Ramsauer-Townsend minimum Q^+_{min} is 6.2×10^{-16} cm^2 at 3.5–5.5 eV. But the position of the minimum is not so clear similar to that in e^+-N_2 and e^+-CO. In the data of Hoffman *et al.*, however, the minimum is shown distinctly at 5.5 eV and $Q^+_{min}=6.1\times10^{-16}$ cm^2. On the other hand, the minimum is not presented clearly in those of Charlton *et al.* Large discrepancies in the energy range lower than 3 eV exist among three measurements similar to the case in e^+-N_2. The fact that very high values of total cross-sections in the low energy range are not shown for e^+-N_2, -CO and -CO_2 in our experiments may be not caused by a systematic error of our apparatus, because very high values in the low energy range for e^+-CH_4, -C_2H_4 and -C_2H_6 (to be submitted) have been presented such as the data of Hoffman *et al.* for e^+-CO_2. More detailed check will be necessary. Though a distinct lobe at the threshold energy of positronium formation has been shown in the data of Charlton *et al.*[10] and Hoffman *et al.*,[8] no lobe was revealed in the present data. Data of Charlton *et al.*, especially, shows a distinct peak at 7 eV with good enough accuracy. Data of the present experiment and those of Charlton *et al.*[22] and those of Kwan *et al.*[9] for e^+-CO_2 in the range from 20 to 400 eV are in fairly good agreement as shown in Fig. 12.

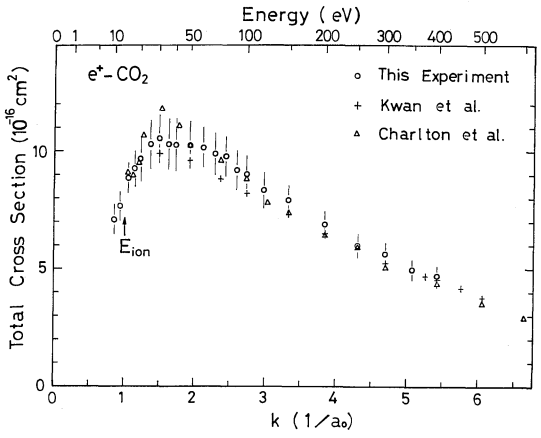

Fig. 12. Total e^+-CO_2 colliding cross-section results extending to intermediate energies. The present results are shown with the experimental data of Kwan *et al.* (ref. 9) and Charlton *et al.* (ref. 22). The threshold of ionization is shown by an arrow.

Values of the total cross-sections for electrons with energies in the range from 5 to 403 eV colliding with CO_2 are given in Fig. 13 along with data of Kwan *et al.*[9] The present data are fairly smaller than those of Kwan

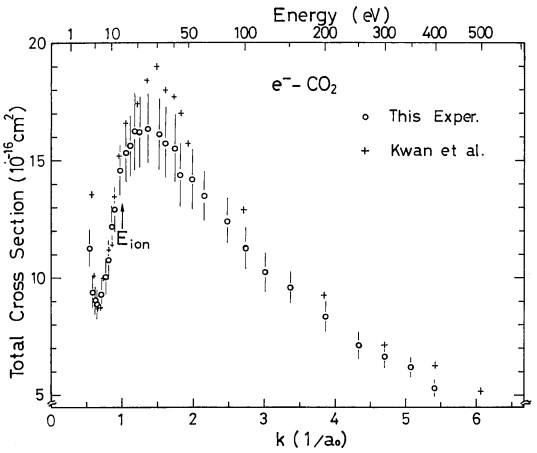

Fig. 13. Total e^--CO_2 colliding cross-section results extending to intermediate energies. The present results are shown with the experimental data of Kwan *et al.* (ref. 9). The threshold of ionization is indicated by an arrow.

et al. This discrepancy can't be explained. The total cross-sections for low-energy electrons have been obtained by many workers with interest in the shape resonance. Data of the cross-sections in the energy range lower than 5 eV are presented in Fig. 7(c) with those of Hoffman *et al.*,[8] of Szmytkowski *et al.*,[29] of Ferch *et al.*[31] and theoretical data of Morrison *et al.*[32] The shape resonance was not quantitatively detected. Except the resonance, data of the electron-collision measurement by our simple method are useful for the comparison with those of the positron collision.

The authors would like to thank to Professor Hiroshi Tanaka for helpful discussions in electron collisions.

References

1) D. G. Costello, D. E. Groce, D. F. Herring and J. W. McGowan: Phys. Rev. B **5** (1972) 1433.
2) K. F. Canter, P. G. Coleman, T. C. Griffith and G. R. Heyland: J. Phys. B **5** (1972) L167.
3) T. C. Griffith and G. R. Heyland: Phys. Report **39** (1978) 170.
4) T. C. Griffith: Adv. in At. and Mol. Phys. **15** (1979) 135.
5) T. S. Stein and W. E. Kauppila: Adv. in At. and Mol. Phys. **18** (1982) 53.
6) W. E. Kauppila and T. S. Stein: Can. J. Phys. **60** (1982) 471.
7) O. Sueoka: J. Phys. Soc. Jpn. **51** (1982) 2381.
8) K. R. Hoffman, M. S. Dababneh, Y.-F. Hsieh, W. E. Kauppila, V. Pol, J. H. Smart and T. S. Stein: Phys. Rev. A **25** (1982) 1393.
9) Ch. K. Kwan, Y.-F. Hsieh, W. E. Kauppila, S. J. Smith, T. S. Stein, M. N. Uddin and M. S. Dababneh: Phys. Rev. A **27** (1983) 1328.
10) M. Charlton, T. C. Griffith, G. R. Heyland and G. L. Wright: J. Phys. B **16** (1983) 323.
11) J. M. Dale, L. D. Hulett and S. Pendyala: Surf. and Interface Anal. **2** (1980) 199.
12) O. Sueoka: Jpn. J. Appl. Phys. **21** (1982) 702.
13) P. G. Coleman, T. C. Griffith, G. R. Heyland and T. R. Twomey: Appl. Phys. **11** (1976) 321.
14) P. G. Coleman, T. C. Griffith and G. R. Heyland: Appl. Phys. **5** (1974) 223.
15) G. Sinapius, W. Raith and W. G. Wilson: J. Phys. B **13** (1980) 4079.
16) H. J. Blaauw, R. W. Wagenaar, D. H. Barends and F. J. de Heer: J. Phys. B **13** (1980) 359.
17) J. W. Darewych and P. Baille: J. Phys. B **7** (1974) L1.
18) E. S. Gillespie and D. G. Thompson: J. Phys. B **8** (1975) 2858.
19) J. W. Darewych: J. Phys. B **15** (1982) L415.
20) M. Charlton, T. C. Griffith, G. R. Heyland, K. S. Lines and G. L. Wright: J. Phys. B **13** (1980) L757.
21) M. Charlton, C. Clark, T. C. Griffith and G. R. Heyland: J. Phys. B **16** (1983) L465.
22) M. Charlton, T. C. Griffith, G. R. Heyland and G. L. Wright: J. Phys. B **13** (1980) L353.
23) J. Dutton, C. J. Evans and H. L. Mansour: *Abst. of VIth Int. Conf. Positron Annihilation* (1982) 82.
24) P. G. Coleman, T. C. Griffith and G. R. Heyland: Appl. Phys. **4** (1974) 89.
25) G. Dalba, P. Fornasini, R. Grisenti, G. Ranieri and A. Zecca: J. Phys. B **13** (1980) 4695.
26) R. E. Kennerly: Phys. Rev. A **21** (1980) 1876.
27) N. Chandra and A. Temkin: Phys. Rev. A **13** (1976) 188.
28) M. S. Dababneh, W. E. Kauppila, J. P. Downing, F. Laperriere, V. Pol, J. H. Smart and T. S. Stein: Phys. Rev. A **22** (1980) 1872.
29) C. Szmytkowski and M. Zubek: Chem. Phys. Lett. **57** (1978) 105.
30) N. Chandra: Phys. Rev. A **16** (1977) 80.
31) J. Ferch, C. Masche and W. Raith: J. Phys. B **14** (1981) L97.
32) M. A. Morrison, N. F. Lane and L. A. Collins: Phys. Rev. A **15** (1977) 2186.